



Influence of Nanoscale Structuralisation on the Catalytic Performance of ZIF-8: A Cautionary Surface Catalysis Study

Journal:	<i>CrystEngComm</i>
Manuscript ID	CE-ART-05-2018-000746.R1
Article Type:	Paper
Date Submitted by the Author:	20-Jul-2018
Complete List of Authors:	Linder-Patton, Oliver; The University of Adelaide, Department of Chemistry de Prinse, Thomas; The University of Adelaide, Chemistry Furukawa, Shuhei; Kyoto University, Institute for Integrated Cell-Material Sciences Bell, Stephen; University of Adelaide, Department of Chemistry Sumida, Kenji; University of Adelaide, Centre for Advanced Nanomaterials Doonan, Christian; The University of Adelaide, School of Chemistry & Physics Sumbly, Christopher; The University of Adelaide, Chemistry



Influence of Nanoscale Structuralisation on the Catalytic Performance of ZIF-8: A Cautionary Surface Catalysis Study

Oliver M. Linder-Patton,^a Thomas J. de Prinse,^a Shuhei Furukawa,^b Stephen G. Bell,^a Kenji Sumida,^a Christian J. Doonan^{a*} and Christopher J. Sumby^{a*}

Received 00th January 20xx,
Accepted 00th January 20xx

DOI: 10.1039/x0xx00000x

www.rsc.org/

Although metal-organic frameworks (MOFs) have been shown to catalyse a wide range of reactions, understanding the influence of nanoscale structuralisation (*e.g.* crystal size and morphology) on their performance is a difficult challenge. Here, we have prepared Zn(2-mIM)₂ (ZIF-8; 2-mIM⁻ = 2-methylimidazolate) crystals of varied size and morphology, and studied the catalytic properties of these samples in the context of the transesterification of vinyl acetate with hexanol. ZIF-8 has previously been shown to catalyse reactions at Lewis acidic sites at the crystal surface and at defect sites. The substrates were selected as they are significantly larger than the pore apertures, allowing the reaction to be confined to the surface of the crystals and providing the best opportunity to understand the influence of the structuralisation on the observed properties. In this case, the rate of hexyl acetate production increased as the crystal size was reduced; however, the effect of crystal morphology on the rate of reaction was not appreciable due to the instability of ZIF-8 under catalytic conditions. It was clearly observed that the surface of ZIF-8 was unstable in catalytic conditions featuring hydrophobic reagents with a polar functional groups, with scanning electron microscopy (SEM) revealing indiscriminate etching of all crystal surfaces. Atomic adsorption spectrometry (AAS) analyses confirmed the etching led to significant leaching of Zn²⁺, which was observed to contribute considerably to the catalytic activity of ZIF-8. Our results highlight the need for fundamental characterisation of MOF catalysts to enable their deployment under a wider variety of catalytic conditions.

Introduction

The catalytic properties of metal-organic frameworks (MOFs) have attracted increased attention in recent years.¹⁻³ The modular synthesis of MOFs, from a combination of organic linkers and metal nodes,⁴ imbues these materials with features that are highly desired for catalysis including; large surface areas, high substrate adsorption capacity and chemical tunability with respect to their internal pore environment.^{4, 5} As such, MOFs can act as heterogeneous catalysts *via* an intrinsic activity stemming directly from the metal nodes/organic ligands, or by supporting catalytic moieties that resemble their homogeneous counterparts.⁵⁻¹⁰ MOFs have been shown to catalyse a broad range of reactions. Both the Knoevenagel condensation¹¹ and Suzuki coupling reactions have been catalysed by MOFs for fine chemical synthesis,^{12, 13} while industrially relevant reactions such as esterification,¹⁴ transesterification,⁷ and ethylene oligomerization reactions

have also been explored.^{15, 16}

Crystal size and morphology have been shown to impact the physical properties of MOFs.¹⁷ Crystal size can affect the framework flexibility,¹⁸⁻²⁰ and even the rate at which a "structurally-locked" framework recovers its flexibility.²¹ Meanwhile, modulators used to control crystal morphology, and which remain bound to crystal surfaces, can alter guest adsorption throughout the pores and at the crystal surface.^{22, 23} In the context of heterogeneous catalysis, control over the crystal size is expected to be crucial for optimising the diffusion path lengths for both reactant and product molecules and for varying ratio between external and internal surface areas.²⁴ Additionally, tuning the crystal morphology can alter the ratios between exposed crystal facets, which could potentially enhance catalytic performance by increasing the density of active sites at the surface of the MOF.²⁵ Despite its potential to greatly enhance the catalytic performance of MOFs, the effect of nanoscale structuralisation of this type is not well-understood. Therefore, studies that probe the effects of such modifications on the catalytic properties of MOFs are urgently needed.

The characterisation of MOFs as catalysts is complicated by the fact that the chemical environment available on the crystal surface and within the inner pores is often distinct. As a first step in analysing the influence of crystal size and morphology a system where the catalytic reaction is restricted to the surface is desirable. For example, the Zn(2-mIM)₂ framework (ZIF-8; 2-

^a Department of Chemistry and the Centre for Advanced Nanomaterials, The University of Adelaide, Adelaide, South Australia 5005, Australia. E-mail: christian.doonan@adelaide.edu.au; christopher.sumby@adelaide.edu.au

^b Institute for Integrated Cell-Material Sciences (WPI-iCeMS), Kyoto University, Kyoto, Japan.

Electronic Supplementary Information (ESI) available: ZIF-8 synthesis details, catalytic protocols and details of post-catalysis characterisation. See DOI: 10.1039/x0xx00000xb

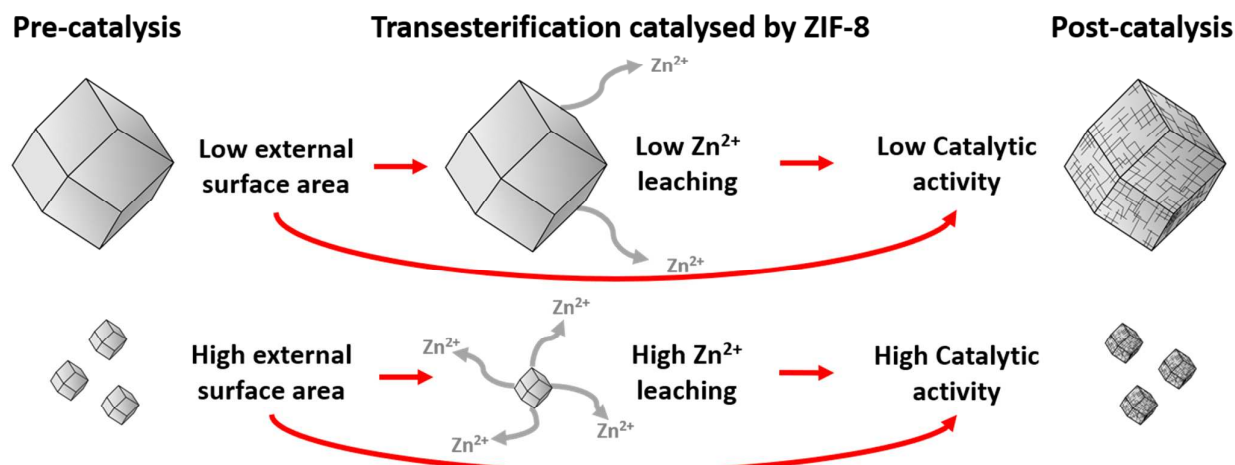


Figure 1. Schematic showing the relationship between particle size and catalytic activity of ZIF-8, with larger crystals having a low external surface area, with fewer active/defect sites for leaching/catalysis to occur, which results in minimal Zn^{2+} leaching and low catalytic activity. Smaller crystals have a correspondingly higher external surface area, with more active/defect sites for leaching/catalysis to occur resulting in higher Zn^{2+} leaching and higher catalytic activity.

mIM⁻ = 2-methylimidazolate), which comprises tetrahedral Zn^{2+} nodes bridged by 2-mIM⁻ linkers to form a sodalite-like structure, has been shown to catalyse a variety of reactions at Lewis acidic sites on its crystal surface, including the transesterification of triglycerides and Knoevenagel condensation reactions.^{7, 11, 26-29} Since the crystallographically measured pore aperture of ZIF-8 is 3.4 Å, in order to probe surface catalysis, a catalytic reaction involving molecules with dimensions significantly larger than this value were used.³⁰ Further, the well-established synthetic protocols for ZIF-8 allow a variety of crystal sizes and morphologies to be obtained while maintaining a high level of crystallinity.^{18, 19, 31}

Herein, we report an investigation into ZIF-8 surface catalysis in the context of model a transesterification reaction, as a function of both crystal size and morphology. Building on established protocols, ZIF-8 was synthesised with a precise control over the crystal size and morphology. Six crystal sizes of ZIF-8 ranging from 50 nm to 100 μm were synthesised. The effect of the crystal morphology was examined specifically at the 500 nm (rhombic dodecahedra and cubic) and 100 μm size regimes (rhombic dodecahedra and truncated rhombic dodecahedron). The catalytic performance of each of the ZIF-8 samples was examined for the transesterification of hexanol and vinyl acetate using two representative experimental protocols (stirred and agitated using a plate shaker/incubator). Interestingly, an increase in the rate of hexyl acetate production was observed with a reduction in crystal size, but the magnitude of the rate increase was smaller than expected based on the difference in external surface areas. This prompted closer examination of the ZIF-8 crystals before and after catalysis, which revealed indiscriminate etching of all of surfaces of the crystal. Furthermore, atomic absorption spectroscopy (AAS) confirmed Zn^{2+} leaching, with smaller crystal sizes being more susceptible to Zn^{2+} release than larger crystals. The amount of Zn^{2+} leached correlated to the catalytic activity of each ZIF-8 particle size regime, with a significant

proportion of the catalytic activity being attributed to Zn^{2+} in solution rather than at the surface of ZIF-8 (Figure 1). Surface etching and Zn^{2+} leaching was also observed for ZIF-8 under conditions in which the Knoevenagel condensation reaction can be catalysed by ZIF-8. In all, these observations indicate that while MOF crystal size and morphology can have considerable influence on the catalyst performance, the characterisation of the activity can be complicated by issues pertaining to stability, transition metal leaching and mechanical degradation. As such, this current study highlights that significant care is required in the characterisation of MOFs as heterogeneous catalysts.

Experimental

General Considerations

All materials were purchased commercially unless otherwise stated. The procedures for synthesis of different crystal sizes and crystal morphologies of ZIF-8 were adapted from literature methods with appropriate modifications, see Table 1 and ESI, section S1.^{18,32, 33} Scanning electron microscopy (SEM) images were collected on a Philips XL30 scanning electron microscope at Adelaide Microscopy. Samples were dry-loaded onto adhesive carbon tabs on aluminium stubs and coated with a 5 nm carbon coating. N_2 (UHP grade, 99.999%) adsorption isotherm measurements were performed on a 3Flex physisorption analyser. The temperature was maintained at 77 K via a Helium cryostat. Powder X-ray diffraction data was collected on a Bruker D8 Advance X-ray powder diffractometer (parallel X-ray, capillary loaded) using a $\text{Cu K}\alpha$ ($\lambda = 1.5418 \text{ \AA}$) radiation source. Samples were mounted in 0.5 mm glass capillaries and data collected for between 2θ of 2° to 52.94° with Φ rotation at 20 rotations/min (1 second exposure per step, 5001 steps). The data were then converted into xye format and background subtracted using WinPlotr 2000 software.³⁴ Simulated powder

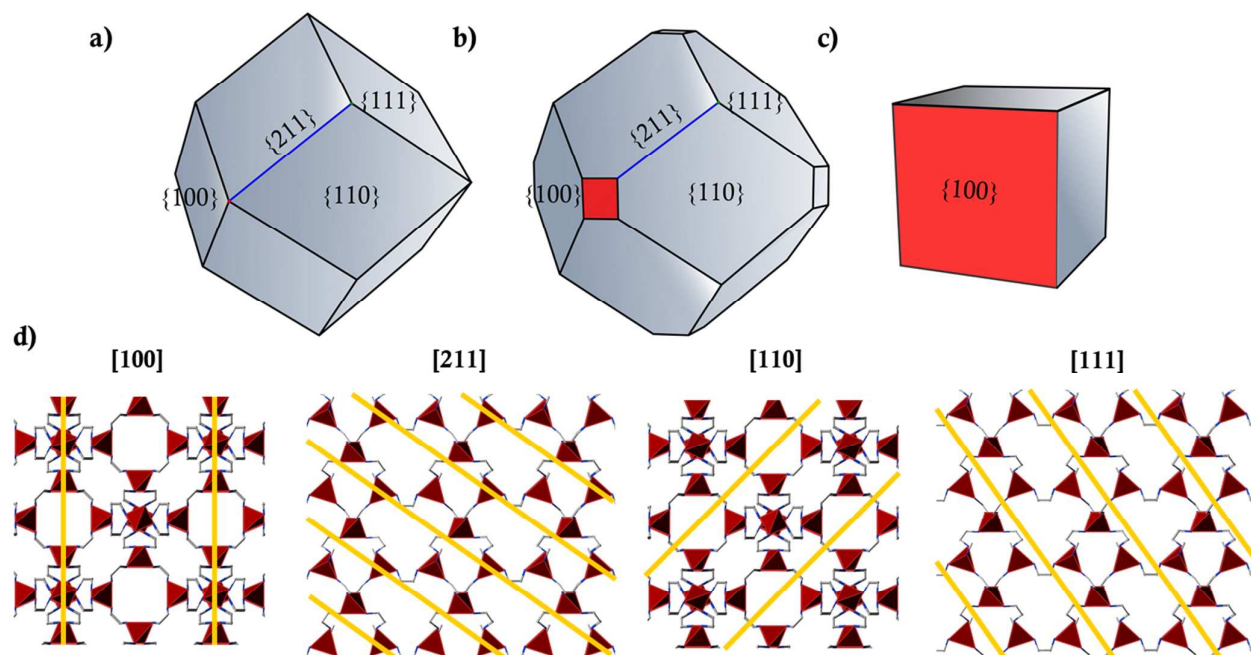


Figure 2. Different morphologies of ZIF-8; a) rhombic dodecahedra, b) truncated rhombic dodecahedra, c) cubic and d) the Miller planes associated with the crystals of ZIF-8. The [100] and [211] planes contain highest density of Zn-2-mIM linkages, indicating that at surfaces corresponding to these Miller planes there will be a high density of Zn(II) centres. The tetrahedral zinc nodes are highlighted in red and the Miller planes are displayed as yellow lines intersecting the crystal lattice.

X-ray diffraction patterns were generated from the single crystal X-ray data using Mercury 3.9.^{35, 36} Atomic adsorption spectroscopy (AAS) measurements were conducted on SpectrAA 250 Phase using a Zinc lamp ($\lambda = 213.9$ nm, slit width 1.0 nm and lamp current 5 mA) with air/acetylene flame fuel source. Gas chromatography mass spectrometry (GC-MS) analyses were carried out on a Shimadzu GC-2010 coupled to a GCMS-QP2010S detector equipped with a DB-5 MS fused silica column (30 m x 0.25 mm, 0.25 μm) using helium as the carrier gas. The oven temperature was held at 50 $^{\circ}\text{C}$ for 2 minutes, then increased at 4 $^{\circ}\text{C min}^{-1}$ to 100 $^{\circ}\text{C}$ and held for 2 minutes, then raised at 30 $^{\circ}\text{C min}^{-1}$ to 220 $^{\circ}\text{C}$ and maintained for 1 minute. The injector and interface temperature were 250 $^{\circ}\text{C}$ and 280 $^{\circ}\text{C}$ respectively.

Catalysis testing

Transesterification (Stirred). The transesterification reaction between hexanol and vinyl acetate, using various crystal sizes and morphologies of ZIF-8 as a catalyst, was carried out in a magnetically stirred round-bottom flask under a N_2 atmosphere. Dried ZIF-8 (20.0 mg, 0.088 mmol, 0.25 wt % relative to vinyl acetate) was dispersed in hexanol (20.0 mL) and heated at 65 $^{\circ}\text{C}$ for 1 h. Vinyl acetate (3.3 mL, 35.79 mmol) was added to the reaction mixture, which was then heated at 65 $^{\circ}\text{C}$ for 6 h. The reaction was monitored by withdrawing 50 μL aliquots from the reaction mixture at different time intervals, these aliquots were centrifuged at 10,000 rpm for 1 minute to separate the ZIF-8 catalyst. An aliquot of the supernatant (15 μL) was transferred to a 2 mL GC-MS vial, the internal standard propyl propionate (16.3 μL , 760 mM in ethyl acetate) was added and the solution was subsequently diluted

to 1.5 mL with ethyl acetate. The solution was then analysed via GC-MS. Catalytic controls including; blank (hexanol + vinyl acetate), 2-mIM, zinc nitrate and mixed controls (2-mIM and zinc nitrate) were conducted (see S2 in the ESI).

Transesterification (Agitated). A modified procedure for the transesterification reaction was conducted in 50 mL sealed conical flasks in a plate shaker/incubator. Dried ZIF-8 (10.0 mg, 0.044 mmol, 0.25 wt % relative to vinyl acetate) was dispersed in hexanol (10.0 mL) and heated at 60 $^{\circ}\text{C}$ for 1 h, agitated at 165 rpm. Vinyl acetate (1.65 mL, 17.89 mmol) was added to the reaction mixture, which was then heated at 60 $^{\circ}\text{C}$ for 6 h. The reaction was monitored via GC-MS in the same manner as described for the stirred reaction above. After the 6 h reaction a 1.5 mL aliquot of the reaction mixture was collected, centrifuged at 10,000 rpm for 1 min. Catalytic controls as detailed above were conducted (see S2 in the ESI).

Knoevenagel condensation (Agitated). Knoevenagel condensation reactions between benzaldehyde and malononitrile using ZIF-8 as the catalyst were carried out in sealed 50 mL conical flasks in a plate shaker/incubator.¹¹ Dried 100 μm ZIF-8 (20.0 mg, 0.088 mmol, 2.5 wt %), benzaldehyde (0.4 mL, 3.8 mmol) were dispersed in a 50 mL conical flask containing toluene (5 mL). A solution of malononitrile (0.5 g, 7.6 mmol) in toluene (5 mL) was then added and the resultant mixture was agitated at room temperature for 6 h at 165 rpm. The ZIF-8 sample was recovered by washing the crystals with toluene and methanol, and the sample was dried under vacuum before SEM analysis. Additionally, controls with neat

toluene, benzaldehyde and malononitrile were conducted with **ZIF-8 100 μm** for etching analysis.

Sample preparation for AAS. Aliquots of the transesterification reaction mixture (0.4 mL) from each stirred reaction were diluted to 20 mL with HNO_3 (3%) and left overnight to extract the zinc into the aqueous layer. The diluted sample was analysed via AAS. Aliquots of the Knoevenagel condensation reaction mixture (0.2 mL) from each stirred reaction were diluted to 20 mL with HNO_3 (3%) and left overnight to extract the zinc into the aqueous layer. The diluted sample was analysed via AAS.

Results and discussion

The catalytic activity of ZIF-8 arises from Lewis acidic sites on the surface of the crystal and at defect sites.⁷ This was recently confirmed via super-resolution fluorescence microscopy, which showed that the acid-base hydrolysis of fluorescein diacetate occurred only on the outer surface of ZIF-8 crystals or at defect sites on the surface.³⁷ Lewis acidic sites on the surface of ZIF-8 are localised on crystal facets that contain metal-ligand linkages at the immediate surface, and their concentration is significantly influenced by the crystal morphology. In this context, the facets representing the [100] and [211] planes are expected to enhance the catalytic reaction via a higher concentration of Lewis acidic sites (Figure 2).³³ The crystal size can also be manipulated for ZIF-8, allowing the ratio of Lewis acid sites to total crystal surface area to be fine-tuned. For example, a greater proportion of Lewis acid sites can be exposed in smaller crystals of ZIF-8, which should result in a dramatic acceleration in the reaction rate.^{18, 19, 31} However, while ZIF-8 is broadly considered to be a chemically stable framework (its hydrophobicity conferring reasonable water stability),^{26, 30} changes in the crystal size are likely to impact its chemical stability, particularly under catalytic conditions (see below).

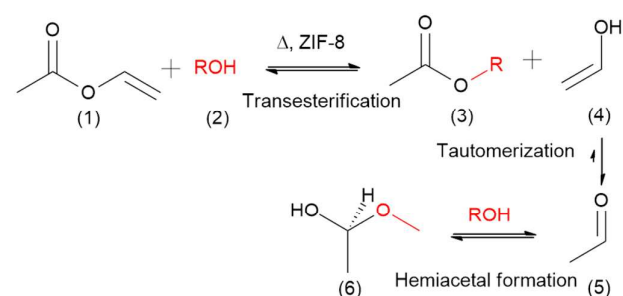
Controlling crystal size and morphology in preparation for ZIF-8 surface catalysis

A systematic investigation of the effect of crystal size and crystal morphology on catalytic activity required the development of robust synthetic protocols for ZIF-8 with control over both attributes. Accordingly, we synthesized ZIF-8 over six discrete crystal sizes ranging from 50 nm to 100 μm with rhombic dodecahedral morphology and at two additional morphologies at 500 nm and 100 μm sizes, as shown in Figure 3 and summarised in Table 1. Crystal size control was achieved through controlled nucleation by varying the Zn^{2+} :2-mIM⁻ molar ratio, the concentration of the modulator,^{18, 31} the counterion in the Zn^{2+} source,³² the reaction solvent, and the temperature.³¹ The crystal size distributions of the ZIF-8 samples were determined via scanning electron microscopy (SEM) (Figure 3 and Figure S1). Note that the synthetic yields for each of the protocols differ significantly, which conceivably is a parameter requiring optimisation prior to scale-up to industrially relevant quantities (grams to kilograms). For

instance, the highest yielding synthesis (**ZIF-8 50 nm**, 76%) was achieved under basic conditions (without modulator) and the lowest yielding protocol (**ZIF-8 10 μm** , 6%) utilised sodium formate as a modulator. The crystallinity and phase purity of the samples was confirmed via PXRD (Figure S2).³⁸

Transesterification catalysis

Transesterification is a reversible reaction that can be catalysed under both acidic and basic conditions.^{39, 40} In order to push the equilibrium in favour of the product an excess of the alcohol is typically used in the presence of a catalyst.³⁹ For the purposes of this study, the transesterification of vinyl acetate was selected because it is effectively a terminating transesterification reaction (Schematic 1). The by-product of the reaction, vinyl alcohol (4), rapidly undergoes tautomerisation to acetaldehyde (5), which reacts with the excess alcohol to form a hemiacetal (6), (see Scheme 1, ESI S3). The effect of crystal size and morphology of ZIF-8 on the surface catalysis of transesterification reactions was analysed by following the reaction between vinyl acetate and hexanol (Scheme 1). Initial testing was conducted at 65 °C with the solution agitated via stirring for 6 h (Figure 4a), and the reaction progress was monitored via GC-MS (Figures S5 and S6).



Scheme 1. Transesterification of vinyl acetate (1) with an alcohol (2), catalysed by ZIF-8, forming an ester (3) and vinyl alcohol (4), the latter of which rapidly tautomerises to acetaldehyde (5) and goes on to react with excess alcohol forming a hemiacetal (6).

Firstly, it was observed that there is an inverse relationship between crystal size and hexyl acetate production, with **ZIF-8 50 nm** and **ZIF-8 100 μm** generating 154 and 82 mM respectively after 6 h. Under these deliberately chosen, mild catalytic conditions modest conversion (10%) is achieved for the best catalyst (**ZIF-8 50 nm**). In comparison, other studies have achieved almost 100% conversion by utilising higher temperatures, up to 200 °C, and shorter length primary alcohols, such as methanol and ethanol.⁷ Secondly, it was found that crystal morphology had no noticeable impact on catalytic activity, with hexyl acetate production for both morphologies of **ZIF-8 500 nm** and **ZIF-8 100 μm** displaying almost identical production, see ESI Figure S7. Given that this reaction occurs at Lewis acidic sites on the surface of ZIF-8 (Figure 2),³³ a much more dramatic difference in catalytic activity would be expected based on both crystal size and

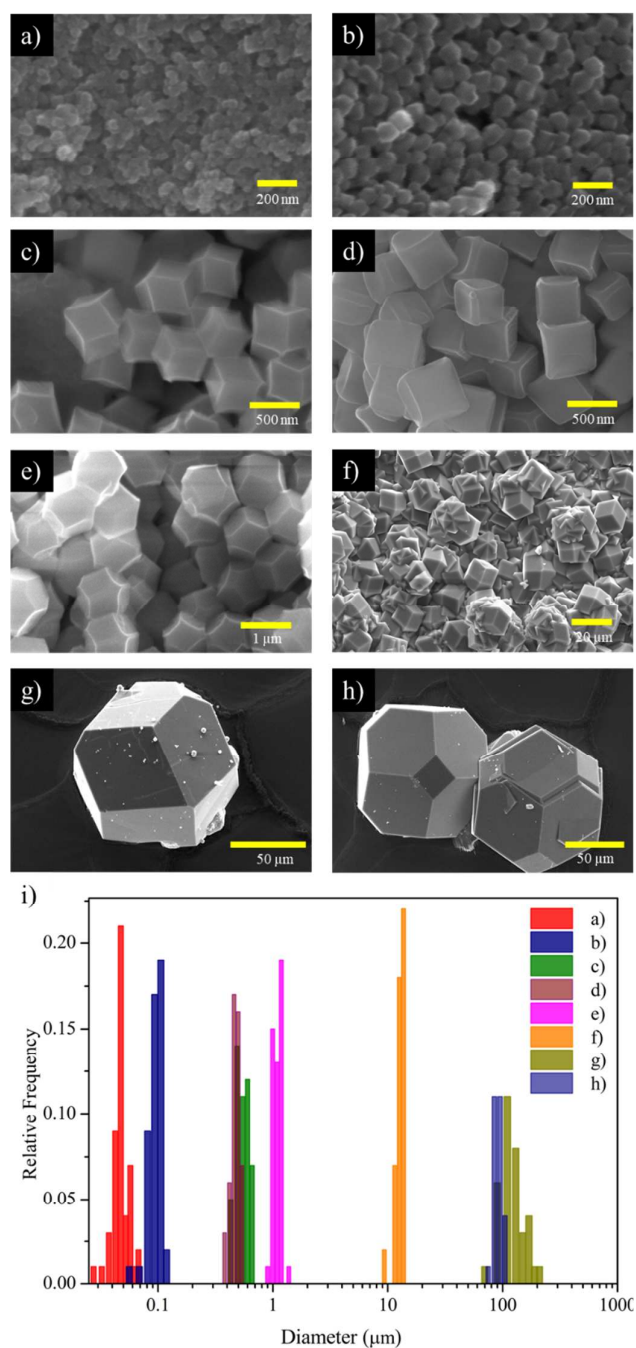


Figure 3. SEM images showing the crystal size and morphology control achieved for ZIF-8 with the corresponding crystal size distributions, all rhombic dodecahedra unless otherwise specified, a) ZIF-8 50 nm, b) ZIF-8 100 nm, c) ZIF-8 500 nm, d) ZIF-8 500 nm cubic, e) ZIF-8 1 μm, f) ZIF-8 10 μm, g) ZIF-8 100 μm, h) ZIF-8 100 μm truncated rhombic dodecahedra and i) crystal size distributions.

Table 1. Detailed synthetic parameters (Zn source, solvent, 2-methylimidazole:Zn ratio, modulator concentration, and temperature), including yields, and morphological characteristics and crystal diameters for all ZIF-8 size regimes.

ZIF-8 sample	Zn source	Solvent (mL)	2-mIM/Zn	Additive/2-mIM (conc.)	Temp. (°C)	Yield (%)	Crystal diameter (μm) ^d	Crystal Morphology	Figure 3 entry
50 nm	Zn(NO ₃) ₂	MeOH (8 mL)	4	0.745 (0.073 M, NaOH)	25	76	0.049 ± 0.001	Rhombic Dodecahedra ^d	a
100 nm	Zn(NO ₃) ₂	MeOH (8 mL)	4	-	25	23	0.093 ± 0.002	Rhombic Dodecahedra	b
500 nm	ZnBr ₂	MeOH (8 mL)	8	-	25	9	0.544 ± 0.009	Rhombic Dodecahedra	c
500 nm cubic	Zn(NO ₃) ₂	H ₂ O (10 mL)	56	0.0001 (0.098 mM, CTAB ^b)	50	73	0.476 ± 0.006	Cubic ^e	d
1 μm	Zn(NO ₃) ₂	MeOH (8 mL)	4	1.000 (0.098 M, 1-mIM ^c)	25	7	1.057 ± 0.013	Rhombic Dodecahedra	e
10 μm	Zn(NO ₃) ₂	MeOH (8 mL)	2	1.000 (0.148 M, HCOONa)	50	10	12.633 ± 0.142	Rhombic Dodecahedra	f
100 μm	Zn(NO ₃) ₂	DMF (8 mL)	0.9	-	140	50	129.945 ± 5.205	Rhombic Dodecahedra	g
100 μm trd	Zn(NO ₃) ₂	MeOH (8 mL)	2	1.122 (0.332 M, HCOONa)	100	6	89.601 ± 1.194	Truncated Rhombic Dodecahedra ^f	h

^a. Average crystal size determined from SEM observations. ^b. Cetyltrimethylammonium bromide. ^c. 1-Methylimidazole. ^d. Rhombic dodecahedra: 12 faces.

^e. Cubic: 6 faces. ^f. Truncated rhombic dodecahedra (trd): 18 faces.

morphology. In fact, there is an inverse power law relationship between crystal size and catalytically active external surface area for ZIF-8; assuming a uniform rhombic dodecahedral morphology (See ESI Figure S8 and Table S2). For example, considering two size regimes of ZIF-8, namely 100 μm and 50 nm, we estimate a 4-million-fold increase in catalytically active external surface area; however, only observe a 2-fold increase in hexyl acetate (mM) produced after a 6 h reaction.

To understand the difference between the predicted and actual catalytic performance, SEM was used to analyse ZIF-8 samples post-catalysis. SEM of ZIF 100 μm post catalysis revealed that there was mechanical degradation of the crystals resulting from the method of agitation (stirring) (Figure 4a, ESI Figure S9), despite crystallinity being retained (Figure S10). The observed fragmentation of ZIF-8 crystals likely increased the amount of catalytically active surface external area available, which corresponded with larger than expected hexyl acetate production for the larger crystal sizes. Additionally, no meaningful contrast between the different morphologies of ZIF-8 could be made because of the crystal degradation under the stirred experimental setup.

To avoid mechanical fragmentation of ZIF-8 crystals, an alternate experimental setup was utilised, with reaction mixture agitated by a plate shaker/incubator (heating at 60 °C, agitated at 165 rpm). Under the modified protocol there was a moderate decrease in catalytic activity across all crystal sizes, attributed to the lower reaction temperature, but the inverse relationship between crystal size and hexyl acetate production was still observed (Figure 4b). As expected, there was a noticeable increase in hexyl acetate production for smaller crystal sizes relative to the ZIF-8 10 μm and ZIF-8 100 μm samples. This outcome indicated that the impact of

mechanical degradation of the crystals on the rate of reaction during the catalysis experiments had been minimised. Again, there was no significant difference in hexyl acetate production for the two distinct morphologies of ZIF-8 500 nm and ZIF 100 μm (see ESI Figure S11). SEM analysis of ZIF 100 μm post-catalysis (agitated) confirmed that no crystal fragmentation had occurred, but instead revealed prominent indiscriminate etching of all facets of the crystal (Figures 4g and S12). Interestingly, partial etching also occurred in the presence of hexanol at 60 °C, although under catalytic conditions the etching was more severe (Figure 4g and S12). Exposing defects on the surface of ZIF-8 crystals increases the number of Lewis acidic sites available for surface catalysis,³⁷ again accounting for the higher than expected activity of ZIF-8 10 μm and ZIF-8 100 μm. 77 K N₂ adsorption isotherms were performed on activated samples of as-synthesised, hexanol treated, and post-catalysis ZIF-8 100 μm, to assess their permanent porosity, (Figure S13 and Table S3) and possible etching-induced macroporosity. Pore size analysis at 77 K with N₂ revealed that there was no notable change in microporosity between the ZIF-8 100 μm samples, nor were macropores identified, indicating that the etching only occurred at the surface of the crystal and no large channels had formed throughout the crystal (Figure S14). The pattern of the crystal surface etching may result from nanometre scale defects on the surface of the crystals, which has been previously observed via *in situ* atomic force microscopy whilst analysing the growth processes of ZIF-8.⁴¹

Given that etching of the crystal surface may lead to Zn²⁺ release, we probed the release of Zn²⁺ post-catalysis by Atomic Absorption Spectroscopy (AAS). By AAS it was found that there was considerable Zn²⁺ leaching for smaller crystal sizes, 16% for ZIF-8 50 nm, relative to larger crystal sizes, 2% for ZIF-8 100 μm (Figure 4h). The extent of Zn²⁺ leaching is proportional to

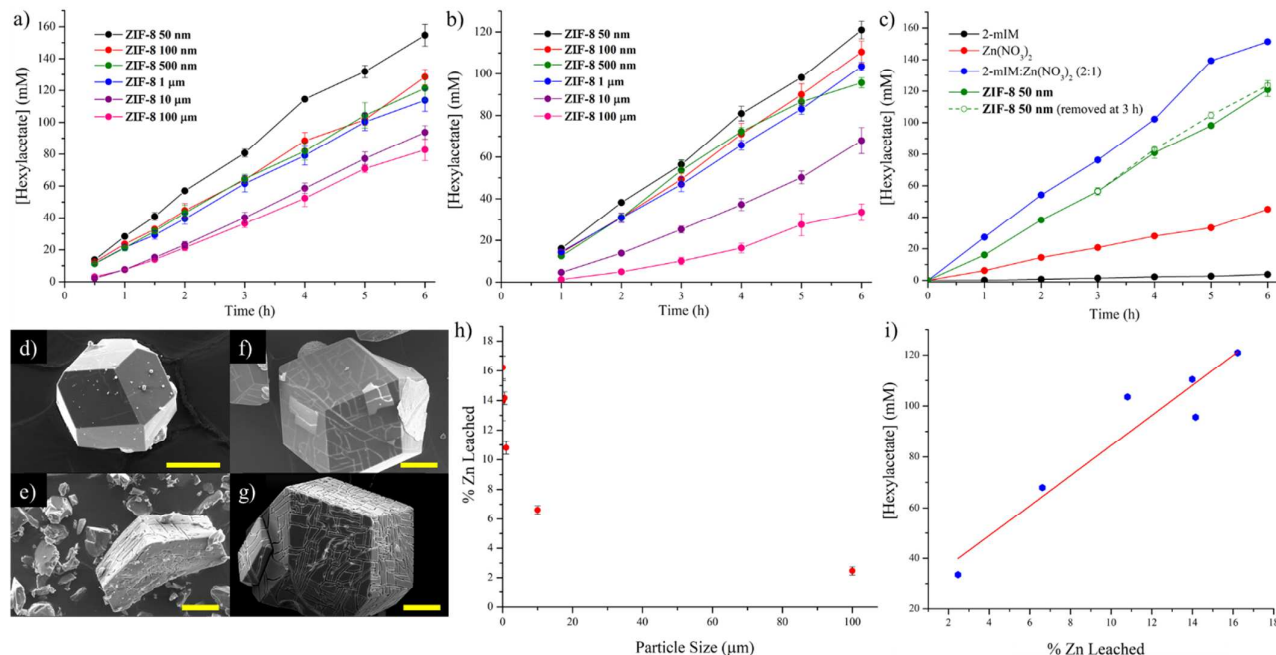


Figure 4. Hexyl acetate production (mM) over a 6 h transesterification reaction between hexanol and vinyl acetate, analysed via GC-MS, catalysed by different crystal sizes of **ZIF-8**; a) reactions heated at 65 °C with stirring agitation, b) reactions heated at 60 °C with shaking agitation and c) catalytic controls including 2-mIM, $\text{Zn}(\text{NO}_3)_2$ and 2-mIM: $\text{Zn}(\text{NO}_3)_2$ (2:1) compared to **ZIF-8 50 nm** (both a 6 h reaction and after 3 h where **ZIF-8** has been removed from solution). SEM images of **ZIF-8 100 μm** d) as-synthesised, e) post-catalysis (stirred), f) agitated in hexanol at 60 °C and g) post-catalysis (agitated). All scale bars represent 50 μm for the SEM images. h) AAS Zn leaching analysis (as a percentage of Zn present in 10 mg of **ZIF-8**) post 6 h of catalysing the transesterification of hexanol with vinyl acetate for all particle sizes. i) A comparison of hexyl acetate production (mM) and % Zn leached post 6 h of catalysing the transesterification of hexanol with vinyl acetate for all particle sizes.

the external surface area of the **ZIF-8** crystals. Since etching of the surface leads to the release of Zn^{2+} and 2-mIM into solution, catalytic controls were conducted with $\text{Zn}(\text{NO}_3)_2$, 2-mIM and a mixture (1:2, $\text{Zn}(\text{NO}_3)_2$:2-mIM). These controls demonstrated that Zn^{2+} and a mixture of Zn^{2+} and 2-mIM catalyse the transesterification reaction (Figure 4c). It is notable that a stoichiometric mixture of Zn^{2+} and 2-mIM (relative to 10 mg of **ZIF-8**) demonstrates significantly higher catalytic activity than Zn^{2+} or 2-mIM alone, indicating a synergistic effect between Zn^{2+} and 2-mIM or some low coordinate $\text{Zn}(\text{2-mIM})$ complex forming in solution to catalyse this reaction. In fact, the Zn^{2+} /2-mIM mixture is more active than **ZIF-8 50 nm**, although this may in part be attributed to poor dispersion under shaking agitation. To determine whether the liberated Zn^{2+} could contribute the observed catalytic activity of **ZIF-8**, an experiment was conducted whereby **ZIF-8 50 nm** was removed (by centrifugation) after 3 h and the progress of the reaction without the solid phase catalyst was followed via GC-MS (Figure 4c). It was observed that the residual Zn^{2+} in solution had equivalent catalytic activity to **ZIF-8 50 nm** after 6 h (Figure 4c). The amount of Zn^{2+} leached at 3 h, was similar to the amount leached after 6 h with **ZIF-8** in solution (15 and 16% respectively as determined by AAS), indicating that the majority of Zn^{2+} leached within the first 3 h of the reaction. Additionally, an interesting relationship was observed between hexyl acetate production and the percentage Zn^{2+} leached after a 6 h reaction, with hexyl acetate production increasing linearly as percentage Zn^{2+}

leached increased (Figure 4i). Decreasing particle size increases the available external surface area which can be etched, releasing increased amounts of Zn^{2+} into solution propagating the catalysis of transesterification reactions. A further ^1H NMR study was conducted to determine whether Zn^{2+} could be released by a smaller chain alcohol such as methanol and be catalytically active (See ESI S3-2 and Table S1). In this experiment the progress of the transesterification of vinyl acetate with $d_4\text{MeOH}$ at 60 °C was monitored via ^1H NMR. 67 – 70% conversion of vinyl acetate to methyl acetate was observed at 3 h and there was 90% conversion at 6 h with **ZIF-8** present. When the solid catalyst was removed after 3 h there was 81% conversion at 6 h, indicating homogeneous catalysis had occurred post-solid catalyst removal (likely resulting from leached Zn^{2+} in solution). Combined these results indicate that (under the conditions used) the catalytic activity of **ZIF-8** is mainly attributed to homogeneous catalysis by release of Zn^{2+} and not to heterogeneous catalysis by active sites on the surface of **ZIF-8**.

Given that the liberated Zn^{2+} /2-mIM contribute significantly to the catalysis of the transesterification of vinyl acetate with hexanol, it is thus challenging to draw concrete conclusions as to the direct impact of crystal size and morphology on surface catalysis with **ZIF-8**, although crystal size directly appears to impact the stability of **ZIF-8**. Importantly, this investigation has highlighted that MOF catalysts, such as **ZIF-8** which are typically thought to be

'robust', are susceptible to surface etching and degradation under liquid phase catalytic conditions.

Surface etching of ZIF-8, both anisotropic and indiscriminate, have been reported previously.^{33, 37} In one example, ZIF-8 crystals were exposed to oleic acid as a means to introduce more defect sites at the surface of the crystals and improve the hydrolysis of fluorescein diacetate.³⁷ Oleic acid is a long chain carboxylic acid with a hydrophobic tail, which likely has high affinity for the hydrophobic surface of ZIF-8. The carboxylic acid group of oleic acid could then bind Zn(II) nodes, potentially liberating Zn²⁺, 2-mIM⁻ and etch the surface of ZIF-8. Hexanol also has a hydrophobic chain, although much shorter than oleic acid, and so the mechanism of etching observed here is presumably similar. Since etching has been observed under catalytic conditions using reagents that have functional groups with an affinity for Zn(II) but are primarily hydrophobic, it would be expected that other reactions with similar reagents might also etch the surface of ZIF-8 and release Zn²⁺/2-mIM⁻. For example, a well-known reaction, catalysed at the surface of ZIF-8, that would be expected to engender surface etching is the Knoevenagel condensation of benzaldehyde and malononitrile.¹¹

Knoevenagel catalytic condition induced surface etching of ZIF-8

The Knoevenagel condensation of benzaldehyde and malononitrile was investigated to determine whether the surface of ZIF-8 was susceptible to etching under other reaction conditions. Given that this is a well-studied reaction for ZIF-8 catalysis,^{11, 26-29} and that the focus of the investigation was to indicate the susceptibility of ZIF-8 to surface etching, a full catalytic study was not undertaken. As such, **ZIF-8 100 μm** samples were studied by SEM to determine whether surface degradation occurred during the Knoevenagel condensation of benzaldehyde with malononitrile.¹¹ The only modification made to the previously used protocol was to avoid mechanical crushing that would occur from stirring; hence the reaction solution was agitated via a plate shaker/incubator at 165 rpm at 25 °C. SEM analysis revealed that **ZIF-8 100 μm** etching occurred when samples were suspended in toluene, or mixtures of toluene/benzaldehyde and toluene/malononitrile, and under catalytic conditions for Knoevenagel condensation (Figure 5). Indiscriminate surface etching was observed in toluene, in the presence of malononitrile and under catalytic conditions, but etching was most severe in the presence of benzaldehyde, with all surfaces appearing noticeably rougher at high magnification than before. Benzaldehyde is hydrophobic and contains a polar functional group (aldehyde), similar to hexanol and oleic acid, which could be expected to etch the surface of ZIF-8 and release Zn²⁺ in a similar manner.

AAS analysis of the samples after 6 h revealed that for toluene and toluene/malononitrile free Zn²⁺ could not be detected. However, for the samples treated with benzaldehyde in toluene and under catalytic conditions,

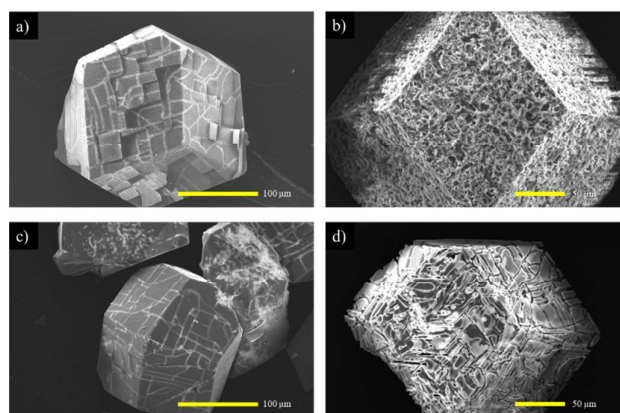


Figure 5. SEM images of **ZIF-8 100 μm** in a) toluene for 6 h, b) benzaldehyde and toluene for 6 h, c) malononitrile and toluene for 6 h and d) under Knoevenagel condensation conditions with malononitrile, benzaldehyde and toluene. All reactions were agitated with a plate shaker/incubator to avoid mechanical degradation of the crystals.

a significant amount of Zn²⁺ was detected in solution: 11.16 ± 0.07 ppm (2% relative to total Zn in 20 mg ZIF-8) and 92.14 ± 0.29 ppm (16%) respectively. PXRD analysis confirmed that the sodalite topology of ZIF-8 was retained post-Knoevenagel condensation catalysis conditions, see ESI Figure S15. While the crystalline structure of ZIF-8 was retained, it has been shown again that the surface of ZIF-8 is not stable under catalytic conditions that feature a hydrophobic reagent with a polar functional group.

Challenges for MOF catalysis

Throughout this investigation we have observed that crystal size has an adverse effect on the stability of ZIF-8 under catalytic conditions (transesterification with hexanol/methanol and Knoevenagel condensation with benzaldehyde), resulting in etching of the crystal surface and leaching of Zn²⁺ and 2-mIM. The etching/Zn²⁺ leaching of ZIF-8 correlates with the amount of the external surface area per crystallite and therefore number of active sites/defects. This trend has also been noted, in part, for the cyclodimerization of epichlorohydrin catalysed at defect sites on ZIF-8, with significant degradation of the crystal surface and a decrease in crystallinity being observed upon recycling the catalyst.⁴² We have also recently reported the effects of crystal size on the rate of structural reorganisation of a "kinetically trapped" phase of a flexible MOF, and noted that the stability of the "kinetically trapped" phase decreased with reduced crystal size.²¹ As well as phase/framework instability under certain conditions, MOFs have been reported to leach transition metals during catalysis (both metals integral to the structure and those appended post-synthetically to a ligand or a defect binding site).^{43, 44} Thus, crystal size likely affects MOF stability during catalysis for other systems as well. As such, appropriate consideration of the catalytic conditions and crystal size regime of candidate MOFs must be given, particularly for materials that are expected to be susceptible to etching/leaching.

Conclusions and Future Outlook

This work examined the catalytic activity of ZIF-8 crystal surfaces for a model transesterification reaction and the crystal surface stability under Knoevenagel condensation reaction conditions. While, as anticipated, improved catalytic performance was observed with decreasing crystal size, the interpretation of this data was complicated by the fact that the ZIF-8 crystal surfaces were indiscriminately etched during catalysis. AAS analysis further confirmed that crystal surface etching is associated with leaching of Zn^{2+} , with the best performing and smallest crystal size regime (50 nm) being most susceptible to this phenomenon. Further analysis revealed that the catalytic activity of ZIF-8 was primarily due to Zn^{2+} leached in solution during catalysis. Similar surface instability was also confirmed for ZIF-8 under catalytic conditions for the Knoevenagel condensation reaction, with significant etching and Zn^{2+} leaching observed. Crystal size appears to have a direct impact on the surface stability of ZIF-8 under catalytic conditions due to the increased external surface of the smaller crystals leading to a proportionally larger number defects/coordination sites being available. For both the surface-based transesterification and Knoevenagel condensation reactions it was observed that ZIF-8 was susceptible to etching by hydrophobic reagents with polar functional groups such as hexanol and benzaldehyde. Although smaller crystal sizes are theoretically more active for surface-based catalysis our observations indicate that crystal size has a greater impact on catalyst stability (and hence reusability). Another outcome of this study is that when investigating MOF catalysis in solution the susceptibility of crystals to undergo changes in their nanoscale structuralisation over time must be carefully considered when assessing catalytic performance.

Acknowledgements

OMLP thanks Matthew Bull for assistance with the Atomic Adsorption Spectrometry measurements, Adelaide Microscopy for access to the XL30 SEM and the Australian Federal Government for a Research Training Program Scholarship. CJS, CJD and KS thank the Australian Research Council for funding (KS: DE160100306; CJD & CJS: DP160103234).

References

1. L. Zhu, X. Q. Liu, H. L. Jiang and L. B. Sun, *Chem. Rev.*, 2017, **117**, 8129-8176.
2. J. Liang, Z. Liang, R. Zou and Y. Zhao, *Adv. Mater.*, 2017, **29**.
3. M. Zhao, K. Yuan, Y. Wang, G. Li, J. Guo, L. Gu, W. Hu, H. Zhao and Z. Tang, *Nature*, 2016, **539**, 76-80.
4. A. Dhakshinamoorthy, M. Alvaro and H. Garcia, *Chem Commun*, 2012, **48**, 11275-11288.
5. P. García-García, M. Müller and A. Corma, *Chem. Sci.*, 2014, **5**, 2979.
6. J. Liu, L. Chen, H. Cui, J. Zhang, L. Zhang and C. Y. Su, *Chem. Soc. Rev.*, 2014, **43**, 6011-6061.
7. C. I. Chizallet, S. Lazare, D. Bazer-Bachi, F. Bonnier, V. Lecocq, E. Soyer, A.-A. Quoineaud and N. Bats, *J. Am. Chem. Soc.*, 2010, **132**, 12365-12377.
8. M. T. Huxley, C. J. Coghlan, W. M. Bloch, A. Burgun, C. J. Doonan and C. J. Sumby, *Philos Trans A Math Phys Eng Sci*, 2017, **375**, 20160028, DOI: 10.1098/rsta.2016.0028.
9. J. D. Evans, C. J. Sumby and C. J. Doonan, *Chem. Soc. Rev.*, 2014, **43**, 5933-5951.
10. M. I. Gonzalez, E. D. Bloch, J. A. Mason, S. J. Teat and J. R. Long, *Inorg. Chem.*, 2015, **54**, 2995-3005.
11. U. P. N. Tran, K. K. A. Le and N. T. S. Phan, *ACS Catalysis*, 2011, **1**, 120-127.
12. H. Fei and S. M. Cohen, *Chem Commun.*, 2014, **50**, 4810-4812.
13. X. Li, R. Van Zeeland, R. V. Maligal-Ganesh, Y. Pei, G. Power, L. Stanley and W. Huang, *ACS Catalysis*, 2016, **6**, 6324-6328.
14. T. Kiyonaga, M. Higuchi, T. Kajiwarra, Y. Takashima, J. Duan, K. Nagashima and S. Kitagawa, *Chem Commun*, 2015, **51**, 2728-2730.
15. M. Gonzalez, J. Oktawiec and J. R. Long, *Faraday Discuss.*, 2017, **201**, 351-367.
16. J. Canivet, S. Aguado, Y. Schuurman and D. Farrusseng, *J. Am. Chem. Soc.*, 2013, **135**, 4195-4198.
17. S. Furukawa, J. Reboul, S. Diring, K. Sumida and S. Kitagawa, *Chem. Soc. Rev.*, 2014, **43**, 5700-5734.
18. C. Zhang, J. A. Gee, D. S. Sholl and R. P. Lively, *J. Phys. Chem. C*, 2014, **118**, 20727-20733.
19. S. Tanaka, K. Fujita, Y. Miyake, M. Miyamoto, Y. Hasegawa, T. Makino, S. Van der Perre, J. Cousin Saint Remi, T. Van Assche, G. V. Baron and J. F. M. Denayer, *J. Phys. Chem. C*, 2015, **119**, 28430-28439.
20. Y. Sakata, S. Furukawa, M. Kondo, K. Hirai, N. Horike, Y. Takashima, H. Uehara, N. Louvain, M. Meilikho, T. Tsuruoka, S. Isoda, W. Kosaka, O. Sakata and S. Kitagawa, *Science*, 2013, **339**, 193-196.
21. O. M. Linder-Patton, W. M. Bloch, C. J. Coghlan, K. Sumida, S. Kitagawa, S. Furukawa, C. J. Doonan and C. J. Sumby, *CrystEngComm*, 2016, **18**, 4172-4179.
22. H. J. Lee, W. Cho, S. Jung and M. Oh, *Adv. Mater.*, 2009, **21**, 674-677.
23. M.-H. Pham, G.-T. Vuong, F.-G. Fontaine and T.-O. Do, *Cryst. Growth Des.*, 2012, **12**, 3091-3095.
24. H. Uehara, S. Diring, S. Furukawa, Z. Kalay, M. Tsotsalas, M. Nakahama, K. Hirai, M. Kondo, O. Sakata and S. Kitagawa, *J. Am. Chem. Soc.*, 2011, **133**, 11932-11935.
25. E. Biemmi, C. Scherb and T. Bein, *J. Am. Chem. Soc.*, 2007, **129**, 8054-8055.
26. Z. Lei, Y. Deng and C. Wang, *J. Mater. Chem. A*, 2018, **6**, 3258-3263.
27. C.-W. Tsai and E. H. G. Langner, *Micropor. Mesopor. Mater.*, 2016, **221**, 8-13.
28. Y.-R. Lee, M.-S. Jang, H.-Y. Cho, H.-J. Kwon, S. Kim and W.-S. Ahn, *Chem. Eng. J.*, 2015, **271**, 276-280.
29. X. Zhao, X. Fang, B. Wu, L. Zheng and N. Zheng, *Sci. Chin. Chem.*, 2013, **57**, 141-146.
30. K. Zhang, R. P. Lively, C. Zhang, R. R. Chance, W. J. Koros, D. S. Sholl and S. Nair, *J. Phys. Chem. Lett.*, 2013, **4**, 3618-3622.
31. Y. Pan, D. Heryadi, F. Zhou, L. Zhao, G. Lestari, H. Su and Z. Lai, *CrystEngComm*, 2011, **13**, 6937.

ARTICLE

Journal Name

32. A. Schejn, L. Balan, V. Falk, L. Aranda, G. Medjahdi and R. Schneider, *CrystEngComm*, 2014, **16**, 4493.
33. C. Avci, J. Arinez-Soriano, A. Carne-Sanchez, V. Guillerm, C. Carbonell, I. Imaz and D. Maspoch, *Angew. Chem. Int. Ed.*, 2015, **54**, 14417-14421.
34. T. Rosinel and J. Rodriguez-Carvajal, *Proceedings of the Seventh European Powder Diffraction Conference (EPDIC 7)*, 2000, 118-123.
35. C. F. Macrae, P. R. Edgington, E. P. P. McCabe, G. P. Shields, R. Taylor, M. Towler and J. v. d. Streek, *J. Appl. Cryst.*, 2006, **39**, 453-457.
36. C. F. Macrae, I. J. Bruno, J. A. Chisholm, P. R. Edgington, E. P. P. McCabe, L. Rodriguez-Monge, R. Taylor, J. v. d. Streek and P. A. Wood, *J. Appl. Cryst.*, 2008, **41**, 466-470.
37. A. Kubarev and M. B. J. Roeffaers, *CrystEngComm*, 2017, **19**, 4162-4165.
38. An additional ZnO phase was observed for ZIF-8 100 μm , likely resulting from the high temperature solvothermal synthetic conditions (140 $^{\circ}\text{C}$, DMF) used for this size regime. It was found that this additional phase persisted despite additional solvent exchange with DMF ($\times 2$) and MeOH ($\times 5$).
39. F. Ataya, M. A. Dube and M. Ternan, *Energy Fuels*, 2007, **21**, 2450-2459.
40. S. Jain, M. P. Sharma and S. Rajvanshi, *Fuel Process. Technol.*, 2011, **92**, 32-38.
41. P. Y. Moh, P. Cubillas, M. W. Anderson and M. P. Attfield, *J. Am. Chem. Soc.*, 2011, **133**, 13304-13307.
42. B. Mousavi, Z. Luo, S. Phatanasri, W. Su, T. Wang, S. Chaemchuen and F. Verpoort, *Eur. J. Inorg. Chem.*, 2017, 4947-4954.
43. J. Gascon, A. Corma, F. Kapteijn and F. X. Llabrés i Xamena, *ACS Catalysis*, 2014, **4**, 361-378.
44. A. Burgun, R. S. Crees, M. L. Cole, C. J. Doonan and C. J. Sumbly, *Chem. Commun.*, 2014, 11760-11763.

TOC text for:

Influence of Nanoscale Structuralisation on the Catalytic Performance of ZIF-8: A Cautionary Surface Catalysis Study

Nanoscale structuralisation is demonstrated to influence the stability and catalytic properties of zeolitic imidazolate framework-8.

